
Translating Diffusion, Wavelets, and Regularisation into Residual Networks

Tobias Alt¹ Joachim Weickert¹ Pascal Peter¹

Abstract

Convolutional neural networks (CNNs) often perform well, but their stability is poorly understood. To address this problem, we consider the simple prototypical problem of signal denoising, where classical approaches such as nonlinear diffusion, wavelet-based methods and regularisation offer provable stability guarantees. To transfer such guarantees to CNNs, we interpret numerical approximations of these classical methods as a specific residual network (ResNet) architecture. This leads to a dictionary which allows to translate diffusivities, shrinkage functions, and regularisers into activation functions, and enables a direct communication between the four research communities. On the CNN side, it does not only inspire new families of nonmonotone activation functions, but also introduces intrinsically stable architectures for an arbitrary number of layers.

1. Introduction

In view of the undeniable success of deep learning approaches in all areas of data science (LeCun et al., 1998; 2015; Schmidhuber, 2015; Goodfellow et al., 2016), there is a strong need to put them on a solid ground by establishing their mathematical foundations.

An *analytic* way towards this ambitious goal is to express successful CNN architectures in terms of well-founded mathematical concepts. However, deep learning offers a plethora of design possibilities, and modern architectures may involve hundreds of layers and millions of parameters. Thus, this way of reducing a highly complex system to a simple and transparent mathematical model is not only very burdensome, but also bears the danger to lose performance of critical CNN features along the way.

¹Mathematical Image Analysis Group, Faculty of Mathematics and Computer Science, Campus E1.7, Saarland University, 66041 Saarbrücken, Germany. Correspondence to: {alt,weickert,peter}@mia.uni-saarland.de

An alternative, *synthetic* way uses well-established models that offer deep mathematical insights to build simple components of neural architectures which inherit these qualities. While this constructive road seems less stony, it has been explored surprisingly little.

In this paper, we follow the road less taken and drive its simplicity to the extreme. Thus, at this point it is not our intention to design highly sophisticated architectures that produce state-of-the-art results in benchmarks. We do not even present any experiments at all.

1.1. Our Contribution

Our goal is to gain theoretical insights that can be useful to suggest neural architectures that are simpler, more compact, involve less parameters, and benefit from provable stability guarantees.

We establish a comprehensive framework that for the first time allows to translate diffusion methods, wavelet approaches, and variational techniques simultaneously into a specific CNN architecture. The reason for choosing three denoising techniques lies in the intrinsic stability of denoising: Noise is a perturbation of the input data, which is not supposed to change the denoised output substantially. To maximise transparency and notational simplicity, we restrict ourselves to the 1D setting and choose particularly simple representatives in each class: Perona–Malik diffusion, Haar wavelet shrinkage, smooth first order variational models, and a single ResNet block. We show that discrete formulations of all three denoising approaches can be expressed as a specific ResNet block. It inherits its stability directly from the three denoising algorithms. Thus, a ResNet consisting only of these blocks is stable for any number of layers.

Whereas typical CNNs learn convolution weights and fix the nonlinear activation function to a simple design, we proceed in the opposite way: We fix the convolution kernels and study various nonlinear activation functions that are inspired by the diffusivities, shrinkage functions, and variational regularisers. For researchers from the diffusion, wavelet or variational communities, this introduces a dictionary that allows them to translate their methods directly into CNN architectures. Deep learning researchers will find

hitherto unexplored nonmonotone activation functions and new motivations for existing ones.

Our results question two architectural principles behind CNNs that are usually taken for granted. One of our findings is the fact that antisymmetric activation functions can occur naturally. More importantly, we also show that nonmonotone activation functions do not contradict even the most restrictive notions of stability and well-posedness.

1.2. Related Work

We see our paper in the tradition of a number of recent contributions to the mathematical foundations of deep learning. For a detailed survey that covers results until 2017, we refer to (Vidal et al., 2017). The following review focuses on works that are relevant for our paper and does not discuss other interesting aspects such as expressiveness (Poggio et al., 2017; Rolnick & Tegmark, 2018; Gribonval et al., 2019) and information theoretic interpretations (Shwartz-Ziv & Tishby, 2017) of CNNs.

The seminal work of (Bruna & Mallat, 2013) employs wavelet operations to come up with scattering networks that perform well on classification problems. This has been the starting point for a number of wavelet-inspired CNNs; see e.g. (Wiatowski & Bölcskei, 2017; Fujieda et al., 2018; Williams & Li, 2018; Rodriguez et al., 2020) and the references therein. Usually they exploit the spectral information or the multiscale nature of wavelets. Our work, however, focuses on iterated shift-invariant wavelet shrinkage on a single scale and utilises its connection to diffusion processes (Mrázek et al., 2005).

Gaining insights into CNNs is possible by studying their energy landscapes (Nguyen & Hein, 2017; Sonoda & Murata, 2017; Chaudhari et al., 2018; Li et al., 2018; Draxler et al., 2018), their optimality conditions (Haeffele & Vidal, 2017), and by interpreting them as regularising architectures (Kukačka et al., 2017; Ulyanov et al., 2018; Dittmer et al., 2020; Kobler et al., 2020). They can also be connected to incremental proximal gradient methods (Kobler et al., 2017; Combettes & Pesquet, 2020; Bibi et al., 2019; Hasannasab et al., 2020), that are adequate for nonsmooth optimisation problems. In the present paper we advocate an interpretation in terms of iterated smooth energy minimisation problems. We do not require proximal steps and can exploit direct connections to diffusion filters (Scherzer & Weickert, 2000; Radmoser et al., 2000).

A prominent avenue to establish mathematical foundations of CNNs is through their analysis in terms of stability. This can be achieved by studying their invertibility properties (Behrmann et al., 2018; Chang et al., 2018), by exploiting sparse coding concepts (Romano et al., 2020), and by inter-

preting deep learning as a parameter identification or optimal control problem for ordinary differential equations (Haber & Ruthotto, 2017; Thorpe & van Gennip, 2019; Zhang & Schaeffer, 2020). CNNs can also be connected to flows of diffeomorphisms (Rousseau et al., 2020) and to parabolic or hyperbolic PDEs (Weinan, 2017; Lu et al., 2017; Li & Shi, 2018; Smets et al., 2020), where it is possible to transfer L^2 stability results (Ruthotto & Haber, 2020). Our work focuses on diffusion PDEs. They allow us to establish stricter stability notions such as L^∞ stability and sign stability.

Within practical settings, connections between PDEs and CNNs are the basis of trainable diffusion models for inverse problems (Chen & Pock, 2016; Arridge & Hauptmann, 2020) and approaches for directly learning PDEs in a data-driven manner (Schaeffer, 2017; Long et al., 2019). We on the other hand specify the PDE directly and analyse its implications on the CNN side. Furthermore, trainable variants of the nonlinearities that we investigate have shown success for traditional models from the fields of diffusion filtering (Barbeiro & Lobo, 2020), wavelet shrinkage (Hel-Or & Shaked, 2008; Schmidt & Roth, 2014; Alt & Weickert, 2020), and regularisation (Kunisch & Pock, 2013; De los Reyes et al., 2017).

We argue for shifting the focus of CNN models towards more sophisticated and also nonmonotone activation functions. The CNN literature offers only few examples of training activation functions (Kligvasser et al., 2018) or designing them in a well-founded and flexible way (Unser, 2019). Nonmonotone activation functions have been suggested already before the advent of deep learning (De Felice et al., 1993; Meilijson & Ruppin, 1994), but fell into oblivion afterwards. We revitalise this idea by providing a natural justification from the theory of diffusion filtering.

1.3. Organisation of the Paper

Our paper is structured as follows. We review general formulations of nonlinear diffusion, wavelet shrinkage, variational regularisation, and residual networks in Section 2. In Section 3, we discuss numerical approximations for three instances of the classical models. We interpret them in terms of a specific residual network architecture, for which we derive explicit stability guarantees. This leads to a dictionary for translating the nonlinearities of the three classical methods to activation functions, which is presented in Section 4. For a selection of the most popular nonlinearities, we derive their counterparts and discuss novel consequences for the design of neural networks in detail. Finally, we summarise our conclusions in Section 5.

2. Basic Approaches

This section sketches nonlinear diffusion, wavelet shrinkage, variational regularisation, and residual networks in a general fashion. For each model, we highlight and discuss its central design choice.

To ensure a consistent notation, all models in this section produce an output signal u from an input signal f . We define continuous one-dimensional signals u, f as mappings from a signal domain $\Omega = [a, b]$ to a codomain $[c, d]$. We employ reflecting boundary conditions on the signal domain boundaries a and b . The discrete signals $\mathbf{u}, \mathbf{f} \in \mathbb{R}^N$ are obtained by sampling the continuous functions at N equidistant positions with grid size h .

2.1. Nonlinear Diffusion

In nonlinear diffusion (Perona & Malik, 1990), filtered versions $u(x, t)$ of an initial signal $f(x)$ are computed as solutions of the nonlinear diffusion equation

$$\partial_t u = \partial_x (g(\partial_x u) \partial_x u) \quad (1)$$

with initial condition $u(x, 0) = f(x)$ and diffusion time t . The evolution creates gradually simplified versions of f . The central design choice lies in the nonnegative, non-increasing, and bounded diffusivity $g(r)$ which controls the amount of smoothing depending on the local structure of the evolving signal. Choosing the constant diffusivity $g(r) = 1$ (Iijima, 1962) leads to a homogeneous diffusion process that smoothes the signal equally at all locations. A more sophisticated diffusivity such as the exponential Perona–Malik diffusivity $g(r) = \exp\left(-\frac{r^2}{2\lambda^2}\right)$ (Perona & Malik, 1990) inhibits smoothing around discontinuities where $|\partial_x u|$ is larger than the contrast parameter λ . This allows discontinuity-preserving smoothing.

2.2. Wavelet Shrinkage

Classical discrete wavelet shrinkage (Donoho & Johnstone, 1994) manipulates a discrete signal \mathbf{f} within a wavelet basis. With the following three-step framework, one obtains a filtered signal \mathbf{u} :

1. *Analysis*: One transforms the input signal \mathbf{f} to wavelet and scaling coefficients by a transformation \mathbf{W} .
2. *Shrinkage*: A scalar-valued shrinkage function $S(r)$ with a threshold parameter θ is applied component-wise to the wavelet coefficients. The scaling coefficients remain unchanged.
3. *Synthesis*: One applies a back-transformation $\tilde{\mathbf{W}}$ to the manipulated coefficients to obtain the result \mathbf{u} :

$$\mathbf{u} = \tilde{\mathbf{W}} S(\mathbf{W} \mathbf{f}). \quad (2)$$

Besides the choice of the wavelet basis, the result is strongly influenced by the shrinkage function $S(r)$. The hard shrinkage function (Mallat, 1999) eliminates all coefficients with a magnitude smaller than the threshold parameter, while the soft shrinkage function (Donoho, 1995) additionally modifies the remaining coefficients equally.

The classical wavelet transformation is not shift-invariant: Transforming a shifted input signal changes the resulting set of coefficients. To this end, cycle spinning was proposed in (Coifman & Donoho, 1995), which averages the results of wavelet shrinkage for all possible shifts of the input signal. This shift-invariant wavelet transformation will serve as a basis for connecting wavelet shrinkage to nonlinear diffusion.

2.3. Variational Regularisation

Variational regularisation (Whittaker, 1923; Tikhonov, 1963) pursues the goal of finding a function $u(x)$ that minimises an energy functional. A general formulation of such a functional is given by

$$E(u) = \int_{\Omega} \left(D(u, f) + \alpha R(u) \right) dx, \quad (3)$$

where a data term $D(u, f)$ drives u towards the input data f , and a regularisation term $R(u)$ enforces smoothness conditions on u . We can control the balance between both terms by the regularisation parameter $\alpha > 0$. A solution minimising the energy is found via the Euler–Lagrange equations (Gelfand & Fomin, 2000). These are PDEs that describe necessary conditions for a minimiser.

A simple yet effective choice for the regularisation term is a first order regularisation of the form $R(u) = \Psi(\partial_x u)$ with a regulariser $\Psi(r)$. The nonlinear function Ψ penalises variations in $\partial_x u$ to enforce a certain smoothness condition on u . Choosing e.g. $\Psi(r) = r^2$ is called Whittaker–Tikhonov regularisation (Whittaker, 1923; Tikhonov, 1963).

2.4. Residual Networks

Residual networks (He et al., 2016) are a popular CNN architecture as they are easy to train, even for a high number of network layers. They consist of chained residual blocks. A residual block is made up of two convolutional layers with biases and nonlinear activation functions after each layer. Each block computes the output signal \mathbf{u} from an input signal \mathbf{f} by

$$\mathbf{u} = \sigma_2(\mathbf{f} + \mathbf{W}_2 \sigma_1(\mathbf{W}_1 \mathbf{f} + \mathbf{b}_1) + \mathbf{b}_2), \quad (4)$$

with discrete convolution matrices $\mathbf{W}_1, \mathbf{W}_2$, activation functions σ_1, σ_2 and bias vectors $\mathbf{b}_1, \mathbf{b}_2$.

The main difference to general feed-forward CNNs lies in the skip-connection which adds the original input signal \mathbf{f}

to the result of the inner activation function. This helps with the vanishing gradient problem and substantially improves training performance.

The crucial difference between residual networks and the three previous approaches is the design focus: The three classical methods consider complex nonlinear modelling functions, while CNNs mainly focus on learning convolution weights and use simple activation functions. We will see that by permitting more general activation functions, we can relate all four methods within a unifying framework.

3. Translation into Residual Networks

Now we are in a position to discuss numerical approximations for the three classical models that allow to interpret them in terms of a residual network architecture.

3.1. From Nonlinear Diffusion to Residual Networks

In practice, the continuous diffusion process is discretised and iterated to approximate the continuous solution $u(x, T)$ for a stopping time T . With the help of the flux function $\Phi(r) = g(r)r$ we rewrite the diffusion equation (1) as

$$\partial_t u = \partial_x (\Phi(\partial_x u)). \quad (5)$$

For this equation, we perform a standard discretisation in the spatial and the temporal domain. This yields an explicit scheme which can be iterated. Starting with an initial signal $\mathbf{u}^0 = \mathbf{f} = (f_i)_{i=1}^N$, the evolving signal \mathbf{u}^k at a time step k is used to compute \mathbf{u}^{k+1} at the next step by

$$\frac{u_i^{k+1} - u_i^k}{\tau} = \frac{1}{h} \left(\Phi \left(\frac{u_{i+1}^k - u_i^k}{h} \right) - \Phi \left(\frac{u_i^k - u_{i-1}^k}{h} \right) \right). \quad (6)$$

Here the temporal derivative is discretised by a forward difference with time step size τ . We apply a forward difference to implement the inner spatial derivative operator and a backward difference for the outer spatial derivative operator. Both can be realised with a simple convolution.

To obtain a scheme which is stable in the L^∞ norm, one can show that the time step size must fulfil

$$\tau \leq \frac{h^2}{2g_{\max}}, \quad (7)$$

where g_{\max} is the maximum value that the diffusivity $g(r) = \frac{\Phi(r)}{r}$ can attain (Weickert, 1998). This guarantees a maximum–minimum principle, stating that the values of the filtered signal \mathbf{u}^k do not lie outside the range of the original signal \mathbf{f} .

To achieve a substantial filter effect, one often needs a diffusion time T that exceeds the stability limit in (7). Then one

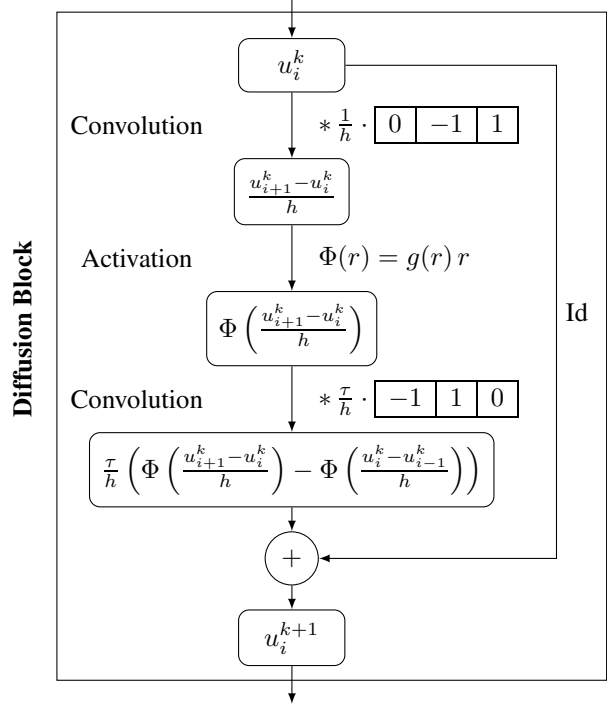


Figure 1. Diffusion block for one explicit nonlinear diffusion step (6) with flux or activation function $\Phi(r)$ and time step size τ . Stencils denote discrete convolution weights centred in position i .

concatenates m explicit steps with a time step size $\tau = \frac{T}{m}$ that satisfies (7).

In order to translate diffusion into residual networks, we rewrite the explicit scheme (6) in matrix-vector form:

$$\mathbf{u}^{k+1} = \mathbf{u}^k + \tau \mathbf{D}_h^- (\Phi(\mathbf{D}_h^+ \mathbf{u}^k)), \quad (8)$$

where \mathbf{D}_h^+ and \mathbf{D}_h^- are convolution matrices denoting forward and backward difference operators with grid size h , respectively. In this notation, the resemblance to a residual block becomes apparent:

Proposition 1. *A diffusion step (8) is equivalent to a residual block (4) if*

$$\sigma_1 = \Phi, \quad \sigma_2 = \text{Id}, \quad \mathbf{W}_1 = \mathbf{D}_h^+, \quad \mathbf{W}_2 = \tau \mathbf{D}_h^-, \quad (9)$$

and the bias vectors $\mathbf{b}_1, \mathbf{b}_2$ are set to $\mathbf{0}$.

We see that the convolutions implement forward and backward difference operators. Crucially, the inner activation function σ_1 corresponds to the flux function Φ . The effect of the skip-connection in the residual block also becomes clear now: It is the central ingredient to realise a time discretisation. We call a block of this form a *diffusion block*.

Figure 1 visualizes such a diffusion block. Graph nodes contain the current state of the signal at position i , while

Table 1. Dictionary for diffusivities $g(r)$, regularisers $\Psi(r)$, wavelet shrinkage functions $S(r)$, and activation functions $\Phi(r)$. A nonlinearity from a row can be translated into a nonlinearity from a column with the respective equation.

to from	Diffusivity	Regulariser	Shrinkage Function	Activation Function
Diffusivity	$g(r)$	$\Psi(r) = 2 \int_0^r g(x) x dx$	$S(r) = r (1 - 4\tau g(\sqrt{2}r))$	$\Phi(r) = g(r) r$
Regulariser	$g(r) = \frac{\Psi'(r)}{2r}$	$\Psi(r)$	$S(r) = r - \sqrt{2}\alpha \Psi'(\sqrt{2}r)$	$\Phi(r) = \frac{1}{2}\Psi'(r)$
Shrinkage Function	$g(r) = \frac{1}{4\tau} \left(1 - \frac{\sqrt{2}}{r} S\left(\frac{r}{\sqrt{2}}\right)\right)$	$\Psi(r) = \frac{1}{4\alpha} \left(r^2 - 2\sqrt{2} \int_0^r S\left(\frac{x}{\sqrt{2}}\right) dx\right)$	$S(r)$	$\Phi(r) = \frac{1}{4\tau} \left(r - \sqrt{2} S\left(\frac{r}{\sqrt{2}}\right)\right)$
Activation Function	$g(r) = \frac{\Phi(r)}{r}$	$\Psi(r) = 2 \int_0^r \Phi(x) dx$	$S(r) = r - 2\sqrt{2}\tau \Phi(\sqrt{2}r)$	$\Phi(r)$

edges describe operations which are applied to proceed from one node to the next.

A related approach for learning parameters of nonlinear diffusion filters in the context of inverse problems has been proposed in (Chen et al., 2015). However, their work establishes a diffusion-reaction framework: The skip-connection rewards similarity to the original image in each step. Therefore, it cannot be translated directly into a residual block (4). On the contrary, we use a pure diffusion model. Our skip-connection rewards similarity to the image from the previous layer and is thus compatible with the residual block formulation.

A consequence of Proposition 1 is that a residual network chaining m diffusion blocks with activation function $\Phi(r)$ and time step size τ approximates a nonlinear diffusion process with stopping time $T = m\tau$ and diffusivity $g(r) = \frac{\Phi(r)}{r}$. These insights enable us to translate a diffusivity g directly into an activation function that coincides with the flux function Φ :

$$\Phi(r) = g(r) r \quad (10)$$

While this translation from a diffusion step to a residual block appears simple, it will serve as the Rosetta stone in our dictionary: It also allows to connect wavelet methods and variational regularisation to residual networks, since both paradigms can be related to diffusion (Mrázek et al., 2005; Scherzer & Weickert, 2000). To keep our paper self-contained, let us now sketch these correspondences.

3.2. From Wavelet Shrinkage to Nonlinear Diffusion

The connection between diffusion PDEs and specific ResNets can be extended to wavelet shrinkage. This is possible due to various equivalence results between diffusion methods and wavelets; see e.g. (Mrázek et al., 2005; Weickert et al., 2006; Ma & Plonka, 2007; Welk et al.,

2008; Dong et al., 2017). In our context, it is sufficient to focus on the results of (Mrázek et al., 2005).

To explore the connection between wavelet shrinkage and nonlinear diffusion, (Mrázek et al., 2005) consider shift-invariant Haar wavelet shrinkage on the finest scale. The missing multiscale structure is compensated by iterating this shrinkage. They show that one step with shrinkage function $S(r)$ is equivalent to an explicit diffusion step with diffusivity $g(r)$, grid size $h = 1$, and time step size τ if

$$g(r) = \frac{1}{4\tau} \left(1 - \frac{\sqrt{2}}{r} S\left(\frac{r}{\sqrt{2}}\right)\right). \quad (11)$$

The L^∞ stability condition (7) from the diffusion case translates into a condition on the shrinkage function

$$-r \leq S(r) \leq r \quad \text{for } r > 0, \quad (12)$$

which is less restrictive than the typical design principle

$$0 \leq S(r) \leq r \quad \text{for } r > 0. \quad (13)$$

Mrázek et al. show that the latter one leads to a sign stable process in the sense of (Schoenberg, 1930), i.e. the resulting signal shows not more sign changes than the input signal. This is a stronger stability notion than L^∞ stability. It limits the time step size to $\tau \leq \frac{h^2}{4g_{\max}}$. This is half the bound of (7).

3.3. From Variational Models to Nonlinear Diffusion

(Scherzer & Weickert, 2000) consider an energy functional with a quadratic data term and a regulariser $\Psi(r)$:

$$E(u) = \int_{\Omega} \left((u - f)^2 + \alpha \Psi(\partial_x u) \right) dx. \quad (14)$$

The corresponding Euler–Lagrange equation for a minimiser u of the functional reads

$$\frac{u - f}{\alpha} = \partial_x \left(\frac{\Psi'(\partial_x u)}{2} \right). \quad (15)$$

Translating Diffusion, Wavelets, and Regularisation into Residual Networks

Table 2. Function plots for selected diffusivities, regularisers, shrinkage functions, and activation functions. The names of known functions are written above the graphs. Bold font indicates the best known function for each row. Axes and parameters are individually scaled for optimal qualitative inspection.

Diffusivity $g(r)$	Regulariser $\Psi(r)$	Shrinkage Function $S(r)$	Activation Function $\Phi(r)$
<p>Constant</p>	<p>Whittaker–Tikhonov</p>		<p>Identity</p>
<p>Charbonnier</p>			
<p>Truncated TV</p>	<p>Huber</p>	<p>Soft</p>	
<p>Perona–Malik</p>			
<p>Truncated BFB</p>		<p>Garrote</p>	
	<p>Truncated Quadratic</p>	<p>Hard</p>	

Table 3. Formulas for the function plots in Table 2. The names of known functions are written above the equations. Bold font indicates the best known function for each row.

Diffusivity $g(r)$	Regulariser $\Psi(r)$	Shrinkage Function $S(r)$	Activation Function $\Phi(r)$
Constant $g(r) = 1$	Whittaker–Tikhonov $\Psi(r) = r^2$	$S(r) = 0$	Identity $\Phi(r) = r$
Charbonnier $g(r) = \frac{1}{\sqrt{1 + \frac{r^2}{\lambda^2}}}$	$\Psi(r) = 2\lambda^2 \sqrt{1 + \frac{r^2}{\lambda^2}} - 2\lambda^2$	$S(r) = r \left(1 - \frac{1}{\sqrt{1 + \frac{2r^2}{\lambda^2}}} \right)$	$\Phi(r) = \frac{r}{\sqrt{1 + \frac{r^2}{\lambda^2}}}$
Truncated TV $g(r) = \begin{cases} 1, & r \leq \sqrt{2}\theta \\ \frac{\sqrt{2}\theta}{ r }, & r > \sqrt{2}\theta \end{cases}$	Huber $\Psi(r) = \begin{cases} r^2, & r \leq \sqrt{2}\theta \\ 2\theta(\sqrt{2} r - \theta), & r > \sqrt{2}\theta \end{cases}$	Soft $S(r) = \begin{cases} 0, & r \leq \theta \\ r - \theta \operatorname{sgn}(r), & r > \theta \end{cases}$	$\Phi(r) = \begin{cases} r, & r \leq \sqrt{2}\theta \\ \sqrt{2}\theta \operatorname{sgn}(r), & r > \sqrt{2}\theta \end{cases}$
Perona–Malik $g(r) = \exp\left(-\frac{r^2}{2\lambda^2}\right)$	$\Psi(r) = 2\lambda^2 \left(1 - \exp\left(-\frac{r^2}{2\lambda^2}\right) \right)$	$S(r) = r \left(1 - \exp\left(-\frac{r^2}{\lambda^2}\right) \right)$	$\Phi(r) = r \exp\left(-\frac{r^2}{2\lambda^2}\right)$
Truncated BFB $g(r) = \begin{cases} 1, & r \leq \sqrt{2}\theta \\ \frac{2\theta^2}{r^2}, & r > \sqrt{2}\theta \end{cases}$	$\Psi(r) = \begin{cases} r^2, & r \leq \sqrt{2}\theta \\ 2\theta^2 \left(\ln\left(\frac{r^2}{2\theta^2}\right) + 1 \right), & r > \sqrt{2}\theta \end{cases}$	Garrote $S(r) = \begin{cases} 0, & r \leq \theta \\ r - \frac{\theta^2}{r}, & r > \theta \end{cases}$	$\Phi(r) = \begin{cases} r, & r \leq \sqrt{2}\theta \\ \frac{2\theta^2}{r}, & r > \sqrt{2}\theta \end{cases}$
$g(r) = \begin{cases} 1, & r \leq \sqrt{2}\theta \\ 0, & r > \sqrt{2}\theta \end{cases}$	Truncated Quadratic $\Psi(r) = \begin{cases} r^2, & r \leq \sqrt{2}\theta \\ 2\theta^2, & r > \sqrt{2}\theta \end{cases}$	Hard $S(r) = \begin{cases} 0, & r \leq \theta \\ r, & r > \theta \end{cases}$	$\Phi(r) = \begin{cases} r, & r \leq \sqrt{2}\theta \\ 0, & r > \sqrt{2}\theta \end{cases}$

This can be regarded as a fully implicit time discretisation for a nonlinear diffusion process with stopping time $T = \alpha$ and diffusivity $g(r) = \frac{\Psi'(r)}{2r}$. This process can also be approximated by m explicit diffusion steps of type (6) with time step size $\tau = \frac{\alpha}{m}$ (Radmoser et al., 2000), where m is chosen such that the stability condition (7) holds.

A related interpretation which is essentially equivalent to the concept of iterated regularisation is given by algorithm unrolling (Kobler et al., 2017; Sulam et al., 2019; Monga et al., 2019).

3.4. Stability Guarantees for Our Residual Network

The connections established so far imply direct stability guarantees for networks consisting of diffusion blocks.

Proposition 2. *A residual network chaining any number of diffusion blocks with time step size τ , grid size h , and antisymmetric activation function $\Phi(r)$ with finite Lipschitz constant L is stable in the L^∞ norm if*

$$\tau \leq \frac{h^2}{2L}, \quad (16)$$

It is also sign stable if the bound is chosen half as large.

Since $\Phi(r) = g(r)r$ and g is a nonincreasing symmetric diffusivity with bound g_{\max} , it follows that $L = g_{\max}$. Thus, (16) is the network analogue of the stability condition (7) for an explicit diffusion step. In the same way, the diffusion block inherits its sign stability from the sign stability condition of wavelet shrinkage. Stability of the full network follows by induction.

Note that our results in terms of L^∞ or sign stability are stricter stability notions than the L^2 stability in (Ruthotto & Haber, 2020) where more general convolution filters are investigated: An L^2 stable network can still produce overshoots which violate L^∞ stability.

Contrary to (Ruthotto & Haber, 2020), our stability result does not require activation functions to be monotone. We will see that widely used diffusivities and shrinkage functions naturally lead to nonmonotone activation functions.

4. Dictionary of Activation Functions

4.1. Main Result

Exploiting the Equations (10), (11), and (15), we are now in the position to present a general dictionary which can be used to translate arbitrary diffusivities, wavelet shrinkage functions, and variational regularisers into activation functions. This dictionary is displayed in Table 1.

On one hand, our dictionary provides a blueprint for researchers acquainted with diffusion, wavelet shrinkage or regularisation to build a residual network for a desired

model while preserving important theoretical properties. This can help them to develop rapid prototypes of the corresponding filters without the need to pay attention to implementational details. Also parallelisation for GPUs is readily available. Last but not least, these methods can be gradually refined by learning.

On the other hand, also CNN researchers can benefit. The dictionary shows how to restrict CNN architectures or parts thereof to models which are well-motivated, provably stable, and can benefit from the rich research results for diffusion, wavelet shrinkage and regularisation. Lastly, it can inspire CNN practitioners to use more sophisticated activation functions, in particular antisymmetric and nonmonotone ones.

4.2. What can We Learn from Popular Methods?

Let us now apply our general dictionary to prominent diffusivities, shrinkage functions, and regularisers in order to identify their activation functions.

We visualise these functions in Table 2 and display their mathematical formulas in Table 3. For our examples, we choose a grid size of $h = 1$. As we have $g_{\max} = 1$ for all cases considered, we set $\tau = \alpha = \frac{1}{4}$. This fulfils the sign stability condition (16).

We generally observe that all resulting activation functions $\Phi(r) = g(r)r$ are antisymmetric, since $g(r) = g(-r)$. This is very natural in the diffusion case, where the argument of the flux function is the signal derivative $\partial_x u$. It reflects a desired invariance axiom of denoising: Signal negation and filtering are commutative.

Still, the discussed antisymmetric activation functions can be expressed with typical ReLU functions (Nair & Hinton, 2010). The truncated total variation activation function

$$\Phi(r) = \begin{cases} r, & |r| \leq \sqrt{2}\theta \\ \sqrt{2}\theta \operatorname{sgn}(r), & |r| > \sqrt{2}\theta \end{cases} \quad (17)$$

provides a simple example as it can be rewritten as

$$\Phi(r) = r - \operatorname{ReLU}(r - \sqrt{2}\theta) + \operatorname{ReLU}(-r - \sqrt{2}\theta). \quad (18)$$

Other activation functions which are not piecewise linear can be approximated with a series of feedforward layers (Hornik et al., 1989). By allowing more advanced antisymmetric activation functions, we can end up with fewer layers. It is surprising that this idea has remained basically unexplored in modern CNNs.

Our six examples in Tables 2 and 3 fall into two classes: The first class comprises diffusion filters with constant (Iijima, 1962) and Charbonnier diffusivities (Charbonnier et al., 1994), as well as soft wavelet shrinkage (Donoho, 1995) which involves a Huber regulariser

(Huber, 1973) and a truncated total variation (TV) diffusivity (Rudin et al., 1992; Andreu et al., 2001). These methods have strictly convex regularisers, and their shrinkage functions do not approximate the identity function for $r \rightarrow \pm\infty$. Most importantly, their activation functions are monotonically increasing. This is compatible with the standard scenario in deep learning where the ReLU activation function dominates (Nair & Hinton, 2010). On the diffusion side, the corresponding increasing flux functions act contrast reducing. Strictly convex regularisers have unique minimisers, and popular minimisation algorithms such as gradient descent converge globally.

The second class is much more exciting. Its representatives are given by Perona–Malik diffusion (Perona & Malik, 1990) and two wavelet shrinkage methods: garrote shrinkage (Gao, 1998) and hard shrinkage (Mallat, 1999). Garrote shrinkage corresponds to the truncated balanced forward–backward (BFB) diffusivity of (Keeling & Stollberger, 2002), while hard shrinkage has a truncated quadratic regulariser which is used in the weak string model of (Geman & Geman, 1984). Approaches of the second class have nonconvex regularisers, which may lead to multiple energy minimisers. Their shrinkage functions converge to the identity function for $r \rightarrow \pm\infty$. The flux function of the diffusion filter is nonmonotone. While this was considered somewhat problematic for continuous diffusion PDEs, it has been shown that their discretisations are well-posed (Weickert & Benhamouda, 1997), in spite of the fact that they may act contrast enhancing. Since the activation function is equivalent to the flux function, it is also nonmonotone. This is very unusual for CNN architectures. Although there were a few very early proposals in the neural network literature arguing that such networks offer a larger storage capacity (De Felice et al., 1993) and have some optimality properties (Meilijson & Ruppim, 1994), they had no impact on modern CNNs.

Our results motivate the idea of nonmonotone activation functions from a different perspective. Since it is well-known that nonconvex variational methods can outperform convex ones, it appears promising to incorporate nonmonotone activations into CNNs in spite of some challenges that have to be mastered.

5. Conclusions

We have seen that CNNs and classical methods have much more in common than most people would expect: Focusing on three classical denoising approaches in a 1D setting and on a ResNet architecture with simple convolutions, we have established a dictionary that allows to translate diffusivities, shrinkage functions, and regularisers into activation functions. This does not only yield strict stability results for specific ResNets with an arbitrary number of layers, but also

suggests to invest more efforts into the design of activation functions. In particular, antisymmetric and nonmonotone activation functions warrant more attention. In our current work, we are investigating their usefulness for prototypical classification problems with CNNs.

Needless to say, our restrictions to 1D, to a single scale, and to denoising methods have been introduced mainly for didactic reasons. We see our work as an entry ticket to guide also other researchers with an expertise on PDEs, wavelets, and variational approaches into the CNN universe. As a result, we envision numerous generalisations, including extensions to higher dimensions and manifold-valued data. Of course, also additional key features of CNNs deserve to be analysed, for instance pooling operations. Our long-term vision is that this line of research will help to bridge the performance gap as well as the theory gap between model-driven and data-driven approaches, for their mutual benefit.

Acknowledgements

This work has received funding from the European Research Council (ERC) under the European Union’s Horizon 2020 research and innovation programme (grant agreement no. 741215, ERC Advanced Grant INCOVID). We thank Michael Ertel for checking our mathematical formulas.

References

- Alt, T. and Weickert, J. Learning a generic adaptive wavelet shrinkage function for denoising. In *Proc. 2020 IEEE International Conference on Acoustics, Speech and Signal Processing*, pp. 2018–2022, Barcelona, Spain, May 2020.
- Andreu, F., Ballester, C., Caselles, V., and Mazón, J. M. Minimizing total variation flow. *Differential and Integral Equations*, 14(3):321–360, March 2001.
- Arridge, S. and Hauptmann, A. Networks for nonlinear diffusion problems in imaging. *Journal of Mathematical Imaging and Vision*, 62:471–487, April 2020.
- Barbeiro, S. and Lobo, D. Learning stable nonlinear cross-diffusion models for image restoration. *Journal of Mathematical Imaging and Vision*, 62:223–237, April 2020.
- Behrmann, J., Dittmer, S., Fernsel, P., and Maass, P. Analysis of invariance and robustness via invertibility of ReLU-networks. arXiv:1806.09730v2 [cs.LG], June 2018.
- Bibi, A., Ghanem, B., Koltun, V., and Ranftl, R. Deep layers as stochastic solvers. In *Proc. 7th International Conference on Learning Representations*, New Orleans, LA, May 2019.

- Bruna, J. and Mallat, S. Invariant scattering convolution networks. *IEEE Transactions on Pattern Analysis and Machine Intelligence*, 35(8):1872–1886, August 2013.
- Chang, B., Meng, L., Haber, E., Ruthotto, L., Begert, D., and Holtham, E. Reversible architectures for arbitrarily deep residual neural networks. In *Proc. 32nd AAAI Conference on Artificial Intelligence*, pp. 2811–2818, New Orleans, LA, February 2018.
- Charbonnier, P., Blanc-Féraud, L., Aubert, G., and Barlaud, M. Two deterministic half-quadratic regularization algorithms for computed imaging. In *Proc. 1994 IEEE International Conference on Image Processing*, volume 2, pp. 168–172, Austin, TX, November 1994.
- Chaudhari, P., Oberman, A., Osher, S., Soatto, S., and Carlier, G. Deep relaxation: partial differential equations for optimizing deep neural networks. *Research in the Mathematical Sciences*, 5(3):30, June 2018.
- Chen, Y. and Pock, T. Trainable nonlinear reaction diffusion: A flexible framework for fast and effective image restoration. *IEEE Transactions on Pattern Analysis and Machine Intelligence*, 39(6):1256–1272, August 2016.
- Chen, Y., Yu, W., and Pock, T. On learning optimized reaction diffusion processes for effective image restoration. In *Proc. 2015 IEEE Conference on Computer Vision and Pattern Recognition*, pp. 5261–5269, Boston, MA, June 2015.
- Coifman, R. R. and Donoho, D. Translation invariant denoising. In Antoine, A. and Oppenheim, G. (eds.), *Wavelets in Statistics*, pp. 125–150. Springer, New York, 1995.
- Combettes, P. L. and Pesquet, J. Deep neural network structures solving variational inequalities. *Set-Valued and Variational Analysis*, February 2020. Online first.
- De Felice, P., Marangi, C., Nardulli, G., Pasquariello, G., and Tedesco, L. Dynamics of neural networks with non-monotone activation function. *Network: Computation in Neural Systems*, 4(1):1–9, 1993.
- De los Reyes, J. C., Schönlieb, C., and Valkonen, T. Bilevel parameter learning for higher-order total variation regularisation models. *Journal of Mathematical Imaging and Vision*, 57(1):1–25, January 2017.
- Dittmer, S., Kluth, T., Maass, P., and Baguer, D. O. Regularization by architecture: A deep prior approach for inverse problems. *Journal of Mathematical Imaging and Vision*, 62:456–470, April 2020.
- Dong, B., Jiang, Q., and Shen, Z. Image restoration: Wavelet frame shrinkage, nonlinear evolution PDEs, and beyond. *Multiscale Modeling and Simulation*, 15(1):606–660, 2017.
- Donoho, D. L. De-noising by soft thresholding. *IEEE Transactions on Information Theory*, 41:613–627, May 1995.
- Donoho, D. L. and Johnstone, I. M. Ideal spatial adaptation by wavelet shrinkage. *Biometrika*, 81(3):425–455, 1994.
- Draxler, F., Veschgini, K., Salmhofer, M., and Hamprecht, F. Essentially no barriers in neural network energy landscape. In Dy, J. and Krause, A. (eds.), *Proc. 35th International Conference on Machine Learning*, volume 80 of *Proceedings of Machine Learning Research*, pp. 1309–1318, Stockholm, Sweden, July 2018.
- Fujieda, S., Takayama, K., and Hachisuka, T. Wavelet convolutional neural networks. arXiv:1805.08620v1 [cs.CV], May 2018.
- Gao, H. Wavelet shrinkage denoising using the non-negative garrote. *Journal of Computational and Graphical Statistics*, 7(4):469–488, December 1998.
- Gelfand, I. M. and Fomin, S. V. *Calculus of Variations*. Dover, New York, 2000.
- Geman, S. and Geman, D. Stochastic relaxation, Gibbs distributions, and the Bayesian restoration of images. *IEEE Transactions on Pattern Analysis and Machine Intelligence*, 6:721–741, 1984.
- Goodfellow, I., Bengio, Y., and Courville, A. *Deep Learning*. MIT Press, Cambridge, MA, 2016.
- Gribonval, R., Kutyniok, G., Nielsen, M., and Voigtlaender, F. Approximation spaces of deep neural networks. arXiv:1905.01208v2 [math.FA], June 2019.
- Haber, E. and Ruthotto, L. Stable architectures for deep neural networks. *Inverse Problems*, 34(1):014004, December 2017.
- Haeffele, B. D. and Vidal, R. Global optimality in neural network training. In *Proc. 2017 IEEE Conference on Computer Vision and Pattern Recognition*, pp. 7331–7339, Honolulu, HI, July 2017.
- Hasannasab, M., Hertrich, J., Neumayer, S., Plonka, G., Setzer, S., and Steidl, G. Parseval proximal neural networks. arXiv:1912.10480v2 [math.NA], April 2020.
- He, K., Zhang, X., Ren, S., and Sun, J. Deep residual learning for image recognition. In *Proc. 2016 IEEE Conference on Computer Vision and Pattern Recognition*, pp. 770–778, Las Vegas, NV, June 2016.

- Hel-Or, Y. and Shaked, D. A discriminative approach for wavelet denoising. *IEEE Transactions on Image Processing*, 17(4):443–457, March 2008.
- Hornik, K., Stinchcombe, M., and White, H. Multilayer feedforward networks are universal approximators. *Neural Networks*, 2(5):359–366, 1989.
- Huber, P. J. Robust regression: Asymptotics, conjectures and Monte Carlo. *The Annals of Statistics*, 1(5):799–821, September 1973.
- Iijima, T. Basic theory on normalization of pattern (in case of typical one-dimensional pattern). *Bulletin of the Electrotechnical Laboratory*, 26:368–388, 1962. In Japanese.
- Keeling, S. L. and Stollberger, R. Nonlinear anisotropic diffusion filters for wide range edge sharpening. *Inverse Problems*, 18:175–190, January 2002.
- Kligvasser, I., Shaham, T. R., and Michaeli, T. xUnit: Learning a spatial activation function for efficient image restoration. In *Proc. 2018 IEEE Conference on Computer Vision and Pattern Recognition*, pp. 2433–2442, Salt Lake City, UT, June 2018.
- Kobler, E., Klatzer, T., Hammernik, K., and Pock, T. Variational networks: Connecting variational methods and deep learning. In Roth, V. and Vetter, T. (eds.), *Pattern Recognition*, volume 10496 of *Lecture Notes in Computer Science*, pp. 281–293. Springer, Cham, 2017.
- Kobler, E., Effland, A., Kunisch, K., and Pock, T. Total deep variation for linear inverse problems. arXiv:2001.05005v2 [math.OA], February 2020.
- Kukačka, J., Golkov, V., and Cremers, D. Regularization for deep learning: A taxonomy. arXiv:1710.10686v1 [cs.LG], October 2017.
- Kunisch, K. and Pock, T. A bilevel optimization approach for parameter learning in variational models. *SIAM Journal on Imaging Sciences*, 6(2):938–983, May 2013.
- LeCun, Y., Bottou, L., Bengio, Y., and Haffner, P. Gradient-based learning applied to document recognition. *Proceedings of the IEEE*, 86(11):2278–2324, November 1998.
- LeCun, Y., Bengio, Y., and Hinton, G. Deep learning. *Nature*, 521:436–444, May 2015.
- Li, H., Xu, Z., Taylor, G., Studer, C., and Goldstein, T. Visualizing the loss landscape of neural nets. In Bengio, S., Wallach, H., Larochelle, H., Grauman, K., Cesa-Bianchi, N., and Garnett, R. (eds.), *Proc. 32nd Annual Conference on Neural Information Processing Systems*, volume 31 of *Advances in Neural Information Processing Systems*, pp. 6389–6399, Montréal, Canada, December 2018.
- Li, Z. and Shi, Z. Deep residual learning and PDEs on manifolds. arXiv:1708.05115v3 [cs.IT], January 2018.
- Long, Z., Lu, Y., and Dong, B. PDE-net 2.0: Learning PDEs from data with a numeric-symbolic hybrid deep network. *Journal of Computational Physics*, 399(2197):108925, December 2019.
- Lu, Y., Zhong, A., Li, Q., and Dong, B. Beyond finite layer neural networks: Bridging deep architectures and numerical differential equations. arXiv:1710.10121 [cs.CV], October 2017.
- Ma, J. and Plonka, G. Combined curvelet shrinkage and nonlinear anisotropic diffusion. *IEEE Transactions on Image Processing*, 16(9):2198–2206, August 2007.
- Mallat, S. *A Wavelet Tour of Signal Processing*. Academic Press, San Diego, second edition, 1999.
- Meilijson, I. and Ruppin, E. Optimal signalling in attractor neural networks. In Tesauro, G., Touretzky, D., and Leen, T. (eds.), *Proc. 7th Annual Conference on Neural Information Processing Systems*, volume 7 of *Advances in Neural Information Processing Systems*, pp. 485–492, Denver, CO, December 1994.
- Monga, V., Li, Y., and Eldar, Y. C. Algorithm unrolling: Interpretable, efficient deep learning for signal and image processing. arXiv:1912.10557v1 [eess.IV], December 2019.
- Mrázek, P., Weickert, J., and Steidl, G. Diffusion-inspired shrinkage functions and stability results for wavelet denoising. *International Journal of Computer Vision*, 64:171–186, September 2005.
- Nair, V. and Hinton, G. E. Rectified linear units improve restricted Boltzmann machines. In *Proc. 27th International Conference on Machine Learning*, pp. 807–814, Haifa, Israel, June 2010.
- Nguyen, Q. and Hein, M. The loss surface of deep and wide neural networks. In Precup, D. and Teh, Y. W. (eds.), *Proc. 34th International Conference on Machine Learning*, volume 70 of *Proceedings of Machine Learning Research*, pp. 2603–2612, Sydney, Australia, August 2017.
- Perona, P. and Malik, J. Scale space and edge detection using anisotropic diffusion. *IEEE Transactions on Pattern Analysis and Machine Intelligence*, 12:629–639, July 1990.

- Poggio, T., Mhaskar, H., Rosasco, L., Miranda, B., and Liao, Q. Why and when can deep - but not shallow - networks avoid the curse of dimensionality: A review. *International Journal of Automation and Computing*, 14 (5):503–519, October 2017.
- Radmoser, E., Scherzer, O., and Weickert, J. Scale-space properties of nonstationary iterative regularization methods. *Journal of Visual Communication and Image Representation*, 11(2):96–114, June 2000.
- Rodriguez, M. X. B., Gruson, A., Polanía, L. F., Fujieda, S., Ortiz, F. P., Takayama, K., and Hachisuka, T. Deep adaptive wavelet network. In *Proc. IEEE Winter Conference on Applications of Computer Vision*, Snowmass, CO, March 2020.
- Rolnick, D. and Tegmark, M. The power of deeper networks for expressing natural functions. In *Proc. 6th International Conference on Learning Representations*, Vancouver, Canada, February 2018.
- Romano, Y., Aberdam, A., Sulam, J., and Elad, M. Adversarial noise attacks of deep learning architectures: Stability analysis via sparse-modeled signals. *Journal of Mathematical Imaging and Vision*, 62:313–327, April 2020.
- Rousseau, F., Drumetz, L., and Fablet, R. Residual networks as flows of diffeomorphisms. *Journal of Mathematical Imaging and Vision*, 62:365–375, April 2020.
- Rudin, L. I., Osher, S., and Fatemi, E. Nonlinear total variation based noise removal algorithms. *Physica D*, 60 (1–4):259–268, November 1992.
- Ruthotto, L. and Haber, E. Deep neural networks motivated by partial differential equations. *Journal of Mathematical Imaging and Vision*, 62:352–364, April 2020.
- Schaeffer, H. Learning partial differential equations via data discovery and sparse optimization. *Proceedings of the Royal Society of London, Series A*, 473(2197): 20160446, January 2017.
- Scherzer, O. and Weickert, J. Relations between regularization and diffusion filtering. *Journal of Mathematical Imaging and Vision*, 12(1):43–63, February 2000.
- Schmidhuber, J. Deep learning in neural networks: An overview. *Neural Networks*, 61:85–117, January 2015.
- Schmidt, U. and Roth, S. Shrinkage fields for effective image restoration. In *Proc. 2014 IEEE Conference on Computer Vision and Pattern Recognition*, pp. 2774–2781, Columbus, OH, June 2014.
- Schoenberg, I. J. Über variationsvermindernde lineare Transformationen. *Mathematische Zeitschrift*, 32:321–328, 1930.
- Shwartz-Ziv, R. and Tishby, N. Opening the black box of deep neural networks via information. arXiv:1703.00810v3 [cs.LG], April 2017.
- Smets, B., Portegies, J., Bekkers, E., and Duits, R. PDE-based group equivariant convolutional neural networks. arXiv:2001.09046v2 [cs.LG], March 2020.
- Sonoda, S. and Murata, N. Double continuum limit of deep neural networks. In *Proc. ICML Workshop on Principled Approaches to Deep Learning*, Sydney, Australia, August 2017.
- Sulam, J., Aberdam, A., Beck, A., and Elad, M. On multi-layer basis pursuit, efficient algorithms and convolutional neural networks. *IEEE Transactions on Pattern Analysis and Machine Intelligence*, March 2019. Online first.
- Thorpe, M. and van Gennip, Y. Deep limits of residual neural networks. arXiv:1810.11741v2 [math.CA], March 2019.
- Tikhonov, A. N. Solution of incorrectly formulated problems and the regularization method. *Soviet Mathematics Doklady*, 4:1035–1038, 1963.
- Ulyanov, D., Vedaldi, A., and Lempitsky, V. Deep image prior. In *Proc. 2018 IEEE Conference on Computer Vision and Pattern Recognition*, pp. 9446–9454, Salt Lake City, UT, June 2018.
- Unser, M. A representer theorem for deep neural networks. *Journal of Machine Learning Research*, 20(110):1–30, 2019.
- Vidal, R., Bruna, J., Giryes, R., and Soatto, S. Mathematics of deep learning. arXiv:1712.04741v1 [cs.LG], December 2017.
- Weickert, J. *Anisotropic Diffusion in Image Processing*. Teubner, Stuttgart, 1998.
- Weickert, J. and Benhamouda, B. A semidiscrete nonlinear scale-space theory and its relation to the Perona–Malik paradox. In Solina, F., Kropatsch, W. G., Klette, R., and Bajcsy, R. (eds.), *Advances in Computer Vision*, pp. 1–10. Springer, Wien, 1997.
- Weickert, J., Steidl, G., Mrázek, P., Welk, M., and Brox, T. Diffusion filters and wavelets: What can they learn from each other? In Paragios, N., Chen, Y., and Faugeras, O. (eds.), *Handbook of Mathematical Models in Computer Vision*, pp. 3–16. Springer, New York, 2006.
- Weinan, E. A proposal on machine learning via dynamical systems. *Communications in Mathematics and Statistics*, 5:1–11, March 2017.

- Welk, M., Steidl, G., and Weickert, J. Locally analytic schemes: A link between diffusion filtering and wavelet shrinkage. *Applied and Computational Harmonic Analysis*, 24:195–224, 2008.
- Whittaker, E. T. A new method of graduation. *Proceedings of the Edinburgh Mathematical Society*, 41:65–75, 1923.
- Wiatowski, T. and Bölcskei, H. A mathematical theory of deep convolutional neural networks for feature extraction. *IEEE Transactions on Information Theory*, 64(3): 1845–1866, November 2017.
- Williams, T. and Li, R. Wavelet pooling for convolutional neural networks. In *Proc. 6th International Conference on Learning Representations*, Vancouver, Canada, February 2018.
- Zhang, L. and Schaeffer, H. Forward stability of ResNet and its variants. *Journal of Mathematical Imaging and Vision*, 62:328–351, April 2020.